Journal of Engineering Physics and Thermophysics, Vol. 75, No. 3, 2002

HIGH-TEMPERATURE-HEAD HYDROAERODYNAMIC HEAT EXCHANGER

O. I. Rakitin

UDC 530.162;536.24

A model of heat exchange and principles of calculation of a hydroaerodynamic heat exchanger (HAHE) on the basis of the theory of locally nonequilibrium processes are presented. The optimum parameters of an HAHE and the principles of its design, which are also true for other mixed locally nonequilibrium systems, have been determined.

In light of recent socioeconomic processes, the problem of conserving the main industrial power resources is of particular importance. In this connection, the hydroaerodynamic heat exchanger holds a certain position. Its operation consists of immersion combustion of a gas-air mixture in an aqueous medium. The combustion temperature is 1200^{o}C. The advantage of this system of heat and mass exchange is the absence of intermediate media for providing heat transfer from the burning gas-air mixture to the aqueous medium. Heat transfer is carried out through direct contact between the media at their interface. The sufficiency of the heat-and-mass exchange surface is determined by the organization of the heat and mass exchange between the immersion-combustion flame and the aqueous medium or, in other words, by the surface of contact between the phase media. This problem is solved through the organization of three stages of heat and mass exchange. Strictly speaking, we are dealing with locally nonequilibrium processes described by the hyperbolic heat-conduction equation [1].

Solving this equation by the method of separation of variables, it is easy to obtain expressions for the propagation of a temperature perturbation in a gas-vapor-air medium

$$\int\limits_{t'_{\text{liq}}}^{t'_{\text{g}}} dt = \int\limits_{0}^{\tau_{\text{r.g}}} (\exp(-\tau/\tau_{\text{r}}) - C_1)\, d\tau \tag{1}$$

or in a liquid medium

$$\int\limits_{t''_{\text{liq}}}^{t''_{\text{g}}} dt = \int\limits_{0}^{\tau_{\text{r.liq}}} (\exp(-\tau/\tau_{\text{r}}) - C_2)\, d\tau\,, \tag{2}$$

where $C_1 = 2a_{\text{g}}\Delta t_{\text{g}}\tau/\delta_{\text{g}}^2$ and $C_2 = 2a_{\text{liq}}\Delta t_{\text{liq}}\tau/\delta_{\text{liq}}^2$ are constants and $\Delta t_{\text{g}} = t'_{\text{g}} - t'_{\text{liq}}$ and $\Delta t_{\text{liq}} = t''_{\text{g}} - t''_{\text{liq}}$ is the temperature head in, respectively, the gas medium and the liquid medium; $\delta_{\text{g}} = \delta_{\text{liq}} = \delta$.

In this case, the temperature change in the gas-vapor-air medium of a gas bubble and in the liquid layer surrounding the bubble will take the form

$$\Delta t_{\text{g}} = \tau_{\text{r}} \frac{\exp(-\tau_{\text{r.g}}/\tau_{\text{r}})}{1 + 2a_{\text{g}}\tau_{\text{r.g}}/\delta_{\text{g}}^2} = \tau_{\text{r}} \frac{\exp(-\tau_{\text{r.g}}/\tau_{\text{r}})}{1 + 2\lambda_{\text{g}}^2/\delta_{\text{g}}^2}\,, \tag{3}$$

Institute of Technical Thermal Physics, National Academy of Sciences of Ukraine, Kiev, Ukraine. Translated from Inzhenerno-Fizicheskii Zhurnal, Vol. 75, No. 3, pp. 156–160, May–June, 2002. Original article submitted January 18, 2001; revision submitted October 9, 2001.

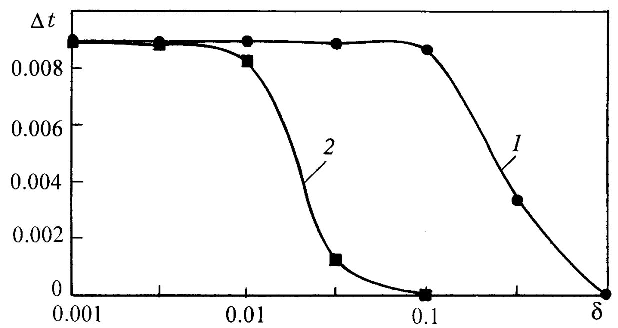

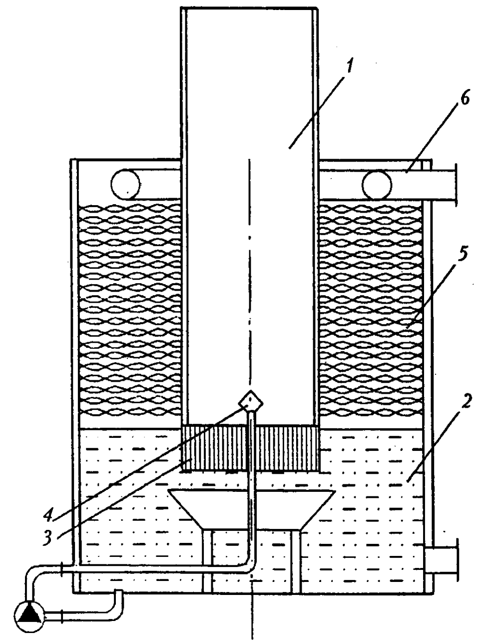

Fig. 1. Dependence of the temperature head Δt (^{o}C) on the length of the conductor δ (mm) at $P = 3000$ Pa: 1) in the gas-vapor-air medium; 2) in the aqueous medium.

Fig. 2. Schematic diagram of a hydroaerodynamic heat exchanger.

$$\Delta t_{\text{liq}} = \tau_{\text{r}} \frac{\exp\left(-\tau_{\text{r.liq}}/\tau_{\text{r}}\right)}{1 + 2a_{\text{liq}}\tau_{\text{r.liq}}/\delta_{\text{liq}}^2} = \tau_{\text{r}} \frac{\exp\left(-\tau_{\text{r.liq}}/\tau_{\text{r}}\right)}{1 + 2\lambda_{\text{liq}}^2/\delta_{\text{liq}}^2}, \tag{4}$$

where $\lambda_{\text{g}} = (a_{\text{g}}\tau_{\text{r.g}})^{0.5}$ and $\lambda_{\text{liq}} = (a_{\text{liq}}\tau_{\text{r.liq}})^{0.5}$ [1, 2].

Figure 1 shows the change in the temperature head as a function of the heated layer δ. It is evident that the temperature head decreases with increase in the thickness of the heated layer. This is explained by the fact that the relaxation times in the liquid and gas-vapor-air media are significantly different because of the different values of the thermal diffisivity in them. Therefore, the heat and mass exchange between the liquid medium and the gas-vapor-air medium of a gas bubble will be determined by the time of relaxation of the latter in the aqueous medium τ_{r}: at $\tau_{\text{r}} > \tau_{\text{r.g}}$ and $\tau_{\text{r}} > \tau_{\text{r.liq}}$ the heat and mass exchange will be the most intense; the gaseous sphere is cooled more rapidly than the water is heated because $\tau_{\text{r.liq}} > \tau_{\text{r}}$. It is evident that the efficiency of the heat exchange is dependent on the total number of gas bubbles, the rate of their formation, and their size: the smaller the size of a gas bubble, the higher the degree of heating of the water layer. However, there is a certain technical limit to the minimum size of a gas bubble. According to Fig. 1, it must be no larger than 1 mm, which is difficult to realize. Because of this, a certain optimum size of a gas bubble d_{sph} is selected, which in turn degrades the characteristics of the heat and mass exchange as a whole, and it becomes necessary to additionally organize the deficient heat-and-mass exchange surface, but on the basis of other principles now.

The above reasoning was used as the basis for the development of a hydroaerodynamic heat exchanger (HAHE) with three stages of heat and mass exchange. Its schematic diagram is presented in Fig. 2.

The exchanger operates in the following way. In the combustion chamber 1, a gas-air mixture at a temperature of 1200^{o}C experiences three stages of heat and mass exchange: the first stage is a water-curtain unit 4, the second (main) stage is a gas-exhaust extension 3 and a bubbling bath 2, and the third stage is a helical heat exchanger 5 and a water-curtain torus 6. The first stage is designed for intensification of heat and mass exchange due to the small length of the transverse heat conductor in the form of a water hood. After the second stage, the temperature of the gas-air mixture is 100^{o}C. The intensification of the heat-and-mass exchange is provided by the optimum size of the cell and by the gas-air-mixture head forming a developed heat-exchange surface. After the third stage, we have

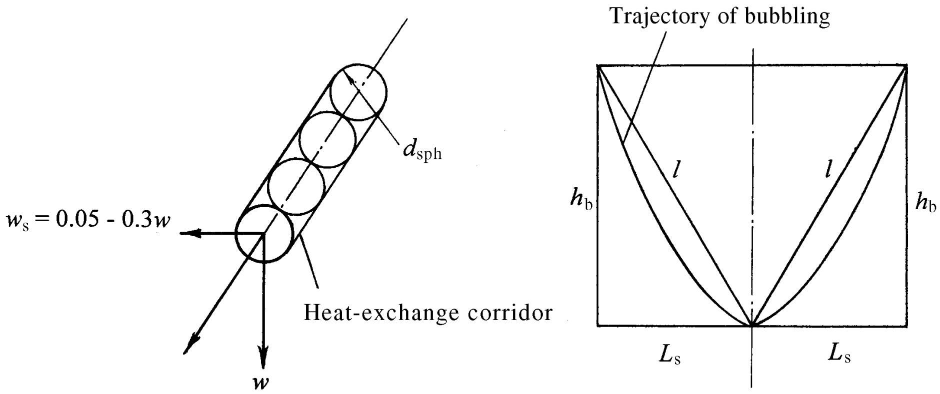

Fig. 3. Model of heat exchange in a bubbling bath.

$t = 45^{o}C$. The intensification of the heat-and-mass exchange is due to the film condensation of water vapor after the second stage on the film surface of water produced by the water-curtain torus 6, on the surface of the helical heat exchanger 5, and in the space between the turns.

The major part of the heat-exchange surface of the HAHE is formed directly by bubbling bubbles of the gas-vapor-air mixture in the aqueous medium at the boundary between the media and is characterized by the direct heat transfer between the media at the sites of their direct contact, the coefficient of diffusion of the water vapor into a gas bubble, and the diffusion mechanisms of condensation and evaporation at the first and third stages of mass exchange. Because of this, apart from the heat wave, there arises a mass wave, and the relation between these waves is determined by the Lewis–Semenov criterion [2, 3].

Let us consider the following model of heat and mass exchange (Fig. 3). A gas-air flow, coming from the small cross section to a larger one, becomes nonuniform in velocity over its cross section. This nonuniformity somewhat decreases in the gas-exhaust extension representing an ordinary grid. The latter, being at the boundary between the gas and liquid media, forms a bubbling flow of the gas-air mixture in the liquid in the form of gas-vapor-air spheres developing the diameter of a grid cell of the gas-exhaust extension and a rotary motion [4]. Since the high-velocity flow is also to a certain degree nonuniform over the cross section of the cell, there arises a moment of forces whose resultant force causes the sphere to shift in the vertical and horizontal planes. As a result, it moves along the parabola until it collapses on the surface of the liquid. To a sufficient degree of approximation, the curvilinear path of motion of the sphere can be replaced by a rectilinear one (Fig. 3). In this case, the length of the path traversed by the sphere is

$$L = 2l = 2\,(L_s^2 + h_b^2)^{0.5} \,. \tag{5}$$

It is evident that

$$L_s = \mu \int_0^w dw \int_0^\tau d\tau = \mu \frac{h_b}{w}\, w = \mu h_b \,, \tag{6}$$

here $\tau = \tau_r$ is the time of action of the buoyancy force on the sphere.

Thus, on the one hand, the sphere is acted upon by the buoyancy force and, on the other, by the forces of the gas-air flow. Consequently, we can determine the depth of bubbling of the sphere

$$\rho_w g F_{eq} \int_0^{h_b} dh = F_{eq} \int_0^P dP \,, \tag{7}$$

where $F_{eq} = \nu F_{ext}$ or $d_{eq} = \nu^{0.5} d_{ext}$; the diameter of the gas-exhaust extension cell coincides with d_{sph} ($d_{eq} = n^{0.5} d_{sph}$).

In this case, the depth of bubbling is

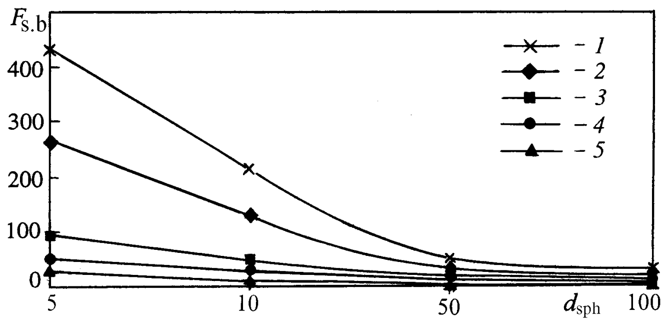

Fig. 4. Dependence of the heat-exchange surface $F_{s.b}$ (m^2) in the bubbling bath on the size of a cell d_{sph} (mm) of the gas-exhaust extension with $d = 0.8$ m in an HAHE of power 1000 kW: 1) $P = 5000$ Pa; 2) 3000; 3) 1000; 4) 500; 5) 300.

$$h_b = \frac{P}{\rho_w g} . \tag{8}$$

After simple manipulations, we obtain

$$L = 2h_b (\mu^2 + 1)^{0.5} = 2 \frac{P}{\rho_w g} (\mu^2 + 1)^{0.5} . \tag{9}$$

On the other hand, the sphere, traveling in the liquid, forms a heat-exchange corridor or a heat-exchange surface of the corridor type since the relaxation time in a liquid or gaseous medium is very large as compared to the time of passage of the sphere through a liquid layer. Assuming that the integral number of spheres of discreteness d_{sph}, traveling along the trajectory L, is

$$M = L/d_{sph} , \tag{10}$$

we have the heat-exchange surface in the bubbling bath

$$F_{s.b} = nMF_{sph} = 2\pi\, nd_{sph}h_b (\mu^2 + 1)^{0.5} \tag{11}$$

or

$$F_{s.b} = \frac{2\pi\, nPd_{sph} (\mu^2 + 1)^{0.5}}{\rho_w g} . \tag{12}$$

Figure 4 shows the change in the heat-exchange surface $F_{s.b}$ as a function of the gas-exhaust extension d_{sph} at different pressures in the combustion chamber.

Consequently, the structure of the heat and mass exchange is determined by the hydroaerodynamics of the gas-air flow in the aqueous medium, and its rate is dependent on the subdivision of this flow into microflows or on the size of the bubbled bubbles. A bubble is properly a sorption space, in whose volume we initially have an intense evaporation. As the bubble travels in the aqueous medium, its temperature decreases and the pressure in it drops.

Thus, the heat-exchange surface is determined by the diameter of an extension cell, the depth of bubbling, or the flow rate of the burning gas-air mixture as well as by the degree of equalization of the flow over the cross section of the combustion chamber. In other words, the rate of formation of rotating spheroids of the gas-vapor-air mixture is determined by the height of the gas-exhaust extension h_{ext}; in this case, the real heat-exchange surface per unit time is

$$I = F_{s.b} w/h_{ext} , \tag{13}$$

which is necessary to determine the design value of h_{ext}.

Such microflows also arise at the first and third stages of heat and mass exchange in the form of a water curtain. In this case, the situation is the same, only instead of a gas bubble in the liquid medium of the second stage of heat and mass exchange we consider a water droplet traveling through the gas-vapor-air medium and developing the diameter of the jet coming out of the water-curtain unit at the first stage of heat and mass exchange or of the water-curtain torus at the third stage of heat and mass exchange, whose entire surface is involved in the process of heat and mass exchange with the microstructure of the burning gas-air mixture at the first stage or the gas-vapor-air mixture after the bubbling bath at the third stage. It should be noted that in one case, the direction of the gas-vapor-air mixture coincides with the direction of the gravitational force, and in the other, they are opposite. Thus, in the first case, the droplet is shifted under the action of the gas-air flow by the distance

$$L_s = \frac{vh}{(w^2 + 2gh)^{0.5}}, \tag{14}$$

and in the second case it is shifted by the distance

$$L_s = \frac{vh}{(w^2 - 2gh)^{0.5}}, \tag{15}$$

here w is the velocity of the gas-vapor-air flow in a given cross section and h is the height of fall of the droplet at the first and third stages of heat and mass exchange.

After simple manipulations, we represent the heat-exchange surface in the following form:

$$F_{\text{cur}} = \frac{n_c \pi P d_c}{\rho_w g} \left[v^2 \left(w^2 \pm \frac{2P}{\rho_w} \right) + 1 \right]^{0.5} \approx \frac{n_c \pi P d_c}{\rho_w g}, \tag{16}$$

here a + sign is used for the water-curtain unit (the first stage of heat and mass exchange) and a – sign is used for the water-curtain torus (the third stage of heat and mass exchange).

The design parameters of the water curtains in an HAHE are selected depending on the design parameters of the second stage (Fig. 4). They form a deficient heat-exchange surface depending on the value of d_{sph}.

Clearly, the total heat-exchange surface is

$$F_1 = F_{\text{s.b}} + F_{\text{cur1}} + F_{\text{cur3}} + F_t. \tag{17}$$

These principles were developed and adopted at the Factory of Building Structures of the State Integrated Civil-Engineering Works of the Administrative Department of the Supreme Soviet of Ukraine in 1998 [5–7]. They have been embodied in a number of thermal contact plants of power from 300 to 1000 kW, which make it possible to save as much as 30% of the main power resources as compared to conventional heat sources, which first of all influences the manufacturing cost of products produced at the enterprise. The HAHE proposed is designed for production of a vapor used for steam curing of reinforced concrete as well as hot water for interior heating of the enterprise. Analog control is used for regulating the power of the device. As a result of the full-scale tests of the HAHE, we have obtained the following technical parameters of its operation: power $W = 350$–1200 kW, operating power $W = 1000$ kW, flow rate of the gas $G_g = 34$–$112\ \text{m}^3/\text{h}$, flow rate of the air $G_{\text{air}} = 340$–$1120\ \text{m}^3/\text{h}$, operating temperature of the vapor-gas mixture for technological steam curing of reinforced concrete $t = 70$–90°C, the operating temperature of the hot water for interior heating of the integrated works $t = 70$–90°C, the temperature of the vapor-gas-air mixture discharged into the atmosphere is $45\ ^{\circ}$C, the combustion temperature of the gas $t = 1200^{\circ}$C, the flow rate of the water in the water-curtain unit of the first stage of heat and mass exchange $G_w = 8\ \text{m}^3/\text{h}$, and the flow rate of the water in the water-curtain torus $G_w = 5$–$40\ \text{m}^3/\text{h}$. The temperature of the water can be varied in wider limits ($t = 40$–90°C) depending on the required heat load. In this case, the HAHE is used only for interior heating of the integrated works.

The operating conditions developed for a high-temperature-head HAHE are also suitable for a low-temperature HAHE [8] used, in particular, in desiccation of air.

NOTATION

a, thermal-diffusivity coefficient, m^2/sec; d, diameter, m; F, area, m^2; g, free-fall acceleration, m/sec^2; G, flow rate, m^3/h; h, depth, m; I, rate of formation of the heat-exchange surface from the gas-vapor-air medium in the bubbling bath, m^2/sec; L, length, m; l, half trajectory of bubbling in the quadratic approximation, m; n, number of cells in the gas-exhaust extension; n_c, number of cells in the water-curtain unit or the water-curtain torus; P, pressure, Pa; t, temperature, ^oC; v, rate of fall of a droplet, m/sec; w, velocity of the gas-air-mixture flow in the combustion chamber, m/sec; W, power, W; δ, thickness of the heated layer around a gas bubble, m; λ, thermal wavelength, m; μ, degree of nonuniformity of the high-velocity gas-air flow at the exit from the gas-exhaust extension; ν, degree of overlapping of the cross section of the gas-exhaust extension; ρ, density, kg/m^3; τ, relaxation time, sec. Subscripts and superscripts: $'$, temperature perturbation in the gas-vapor-air medium; $''$, the same in the liquid medium; b, bubbling; w, water; air, air; g, gas; cur, water curtain; cur.1, water curtain of the first stage of heat and mass exchange; cur.3, water curtain of the third stage of heat and mass exchange; liq, liquid; c, circuit; ext, gas-exhaust extension; s, horizontal shift of a gas sphere relative to the surface; s.b, heat-exchange surface in the bubbling bath; r, relaxation of a gas bubble in the liquid medium; r.g, relaxation of a temperature perturbation in the gas medium; r.liq, relaxation of a temperature perturbation in the liquid medium; t, helical heat exchanger of the third stage of heat and mass exchange; sph, gas sphere; eq, equivalent, set of outlets of the gas-exhaust extension.

REFERENCES

1. S. L. Sobolev, *Usp. Fiz. Nauk*, **161**, No. 3, 5–29 (1991).
2. O. I. Rakitin, *Vestn. Mezhdunar. Akademii Kholoda*, No. 2, 29–30 (2001).
3. G. A. Mukhachev and V. S. Shchukin, *Thermodynamics and Heat Transfer* [in Russian], Moscow (1991).
4. G. Smirnov, *Birth of a Vortex* [in Russian], Moscow (1982).
5. *Thermal Plant*, Ukrainian Patent No. 98020608, MKI 6 F 24H 1/10, 19.02.1999; Byul. No. 2.
6. *Thermal Plant*, Ukrainian Patent No. 98095150, MKI 6 F 24H 1/10, 15.12.2000; Byul. No. 7-II.
7. *Contact Thermal Plants UTK*, Specs. 21631667.001-98, Ukraine.
8. A. Aziz and V. J. Lunardini, *Int. Commun. Heat Mass Transfer*, **18**, 813–822 (1991).